Improved Parameter Estimation of Triple Diode Photovoltaic systems

Oluwasegun Ajetunmobi
Department of Technology and Software
University of Europe for Applied Sciences
Potsdam, Germany
oluwasegun.ajetunmobi@ue-germany.de

Talha Ali Khan
Department of Technology and Software
University of Europe for Applied Sciences
Potsdam, Germany
talhaali.khan@ue-germany.de

Syed Arslan Abbas Rizvi
Department of Technology and Software
University of Europe for Applied Sciences
Potsdam, Germany
syedarslan.rizvi@ue-germany.de

***Abstract*—The extraction of the parameters of solar photovoltaic models is an optimization problem which is nonlinear, multivariable and complex. In this thesis, six modifications were made to the Improved Whale Optimization Algorithm (IWOA) in order to improve the efficacy of the algorithm. These modifications adopt the properties of algebraic and transcendental functions such that the algorithm's balance between exploration and exploitation can be balanced measurably. Ten experiments were carried out to test each of the six modifications on ten benchmark functions. The results were plotted and statistically analyzed to provide a performance overview. The experimental results demonstrated that the modifications are feasible improvements to the IWOA.**

***Index Terms*—Photovoltaics, Parameter Estimation, Triple Diode, Whale Optimization, Modification**

I. Introduction

In recent decades, the rising population has warranted an up-rise in the demand for electrical energy. This increasing demand for this energy calls for a sustainable solution which will be in a position to cater for the ever-increasing world's population without incurring a lot of environmental damage. Coupled with the rapid depletion of non-renewable energy resources the urgency of developing renewable energy sources has been highlighted among researchers and leading economies. Among these alternatives, solar energy has emerged as a mature and promising option due to its potential to generate electricity and thermal energy without water or fuel consumption, while also minimizing pollution and contributing significantly to ecological improvement [1].

Solar energy is particularly effective in power generation, especially through the use of photovoltaic (PV) technology [2, 3, 4]. Photovoltaic panels, which rely on solar cells (SC), efficiently convert sunlight into electricity in an environmentally friendly and renewable manner. This aspect of solar energy production makes it an attractive option for sustainable energy generation [5].

It is imperative to have accurate modelling of the photovoltaic (PV) cell to optimize the effectiveness and maximize the energy output of solar technologies. The non-linearity in the current-voltage (I-V) behaviour of PV systems often induces difficulties in parameter identification. Hence advanced techniques are inevitable to precisely simulate, performance-assess, and optimize the design of the system. Determining key parameters accurately is pivotal to the complex process of modelling PV cells [6]. The complexity in the modelling process arises from the nonlinear I-V curve and the effects associated with the interaction of PV systems with peculiar facts. To determine such factors as semiconductor materials and electrical characteristics about the interaction of a system with sunlight makes the entire phenomenon utterly complex. Therefore the behavior of PV cells could not be correctly represented by traditional linear models. To cope with such challenges, the researchers and engineers developed advanced algorithms and simulation tools.

The triple-diode model comprises three diode components for different types of recombination processes or loss mechanisms existing in solar cells. Ideally, one diode represents an ideal p-n junction, another diode describes recombination in the depletion region and the third could represent surface or space charge region recombination. This model produces a more sweeping outlook on the nature of the cell, considering cases where part of the cell was shaded or under low light [7]. Even though the triple diode model is primarily used for research and simulation, it still gives a good avenue for researchers to improve the design and efficiency of both solar cells and extraction techniques [8].

In the recent past, the strategies of determining the electrical model parameters have become prominent among metaheuristic algorithms due to their capability of handling linear and complex nonlinear optimization problems without being bound by accurate mathematical model requirements. This thus reduces computational burdens greatly and hence, has been applied widely in PV cell parameter identification [6].

Evolutionary Algorithms (EA) employ adaptive techniques based on natural or biological evolution and natural selection.

Specifically, they engage a randomized process of selection, mutation and recombination to arrive at a globally optimal solution [9]. Due to its robust possibility of applications to research cases, EAs have become an important optimization and search technique in recent decades [10]. Two variants of EAs were considered during the research phase of this thesis: Differential Evolution [11] and Genetic Algorithm [12]. They are effective at estimating parameters but only when all the parameters are tuned to fit the environmental context of the module [12]. Simulated Annealing (SA) was used to estimate the parameters of PV modules. Inspired by the concept of annealing in metallurgy, it transposes ideas like entropy and thermodynamic free energy to create a probabilistic method for approximating the global optima of a search space [13]. In this technique, the parameters are first extracted using conventional methods. Then the uncertainties of each parameter are computed to compact the search space of the parameters. Then the immediate values are determined using the results of the first two considerations. This process was confirmed to be quite effective when compared against other established algorithms [14].

NOMENCLATURE

Φ	Parameter decision vector
A	Current
a	Linearly decreasing parameter
b	constant
$I-V$	Current-Voltage
I_t	Output (Terminal) Current (A)
I_{ph}	Photo-generated Current (A)
I_{sd}	Shunt diode current (A)
I_{sh}	Shunt resistor current (A)
k	Boltzmann constant $(1.3806503 \times 10^{-23} J/K)$
l, p	Random real numbers $\in (0, 1)$
n	Ideality factor of the diode
N_E	Number of samples
P	Power
q	Charge magnitude of an electron $(1.60217646 \times 10^{-19} C)$
R_s	Series resistance (Ω)
R_{sh}	Shunt resistance (Ω)
T	Temperature
t	current iteration
V	Voltage
V_t	Terminal Voltage (V)
x	Function index

Researchers developed the Flower Pollination Optimization Algorithm (FPOA) for parameter estimation in PV cells. This method draws from the behaviour of bees when seeking out flowers for nectar harvesting. In this scenario, the flower positions are considered to be the possible solution locations in the search space, while the amount of nectar they hold becomes the objective function to be maximized [15]. This method was applied to a given TD PV model and was shown to provide a greater performance quality than when applied on SD and DD models, which execute the local and global search protocol within a single jump[16].

Swarm intelligence has been engaged in the extraction of parameters. A frequently occurring example of this is the Particle Swarm Optimization (PSO) which is popularly used for other research cases. The PSO simply initializes particle vectors as search agents in a closed domain which randomly search for the global best solution by adjusting their direction and path relative to the best-performing particle in each iterative step [17]. The PSO was used to align the computed I-V determinants of the PV cells to the experimentally obtained ones [18]. Following this, improvements such as the Fractional Order Darwinian Particle Swarm Optimization have been developed and applied to DD models successfully[19].

The Cat Swarm Optimization (CSO) algorithm has been posited as a way to estimate the unknown parameters of single and double-diode models [20]. The CSO algorithm is induced by the behaviour of cats searching for food as a group and was shown to be an effective tool in optimizing the parameters of SC models.

The Whale Optimization Algorithm (WOA) is a relatively new meta-heuristic optimization algorithm which mimics the helix-shaped hunting behaviour of humpback whales [21, 22] and has been shown to outperform popular choices such as the PSO [23]. It was proposed to analyze and model the PV system while considering both series and shunt resistances to track the MPP of the system [24]. While effective in a general myriad of cases, the WOA was noticed to stagnate when handling multimodal problems as it was seen to not thoroughly examine the entire solution space, leading to stagnation as it has no way to reassess and escape local minima after falling into it [25]. This prompted the development of the Improved Whale Optimization Algorithm (IWOA) which proposed two strategies for prey position acquisition to balance local and global exploitation and exploration respectively [26]. It was shown that the IWOA was better than the original WOA. However, parameter adaptive methods to effectively adjust the coefficient A to enhance the performance of IWOA were remarked as an opportunity for further research [26].

II. METHODOLOGY

A. Model of a PV module

The mathematical model of a solar cell -indicative of the dynamic variables governing the behaviour- sheds more emphasis on the design attributes of the SC by explaining its current and voltage (I-V) relation [27, 28, 29].

These parameters critically affect the performance of the solar cells or photovoltaic (PV) modules. There are three major types of PV modules known by the number of diodes they contain. They are the Single-Diode (SD) model, the Double-Diode (DD) model, and a Triple-Diode (TD) model [30, 31, 32]. The parameters, moreover, are useful to model the inherent non-linearities of the solar cell coupled with properties like photo-generated current, diode saturation current, series resistance and diode ideality factor. In essence, accurate estimation of

TABLE I
PARAMETER DOMAIN RANGE OF SINGLE DIODE MODELS

Parameter	Domain range
$R_s(\Omega)$	(0, 0.5)
$R_{sh}(\Omega)$	(0, 100)
I_{ph} (A)	(0, 1)
I_{sd} (μA)	(0, 1)
n	(1, 2)

these parameters becomes critical in attaining an optimum trade-off between current and voltage.

B. Single-diode model

This is the simplest form of a PV module. It consists of a current source, one diode and two resistors [33] as shown in figure 1:

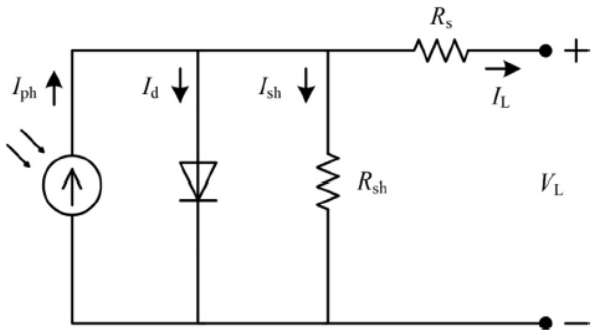

Fig. 1. A single diode circuit model

The output current (I_t) is given by:

$$I_t = I_{ph} - I_{sd} - I_{sh} \tag{1}$$

Where I_t denotes the terminal current and I_{ph}, I_{sd} and I_{sh} being the photo-generated, diode currents and shunt resistor correspondingly. In a more presentable form, making use of the Shockley diode equation we obtain:

$$I_t = I_{ph} - I_{sd}\left[\exp\left(\frac{q(V_t + R_s \cdot I_t)}{n \cdot k \cdot T}\right) - 1\right] - \frac{V_t + R_s \cdot I_t}{R_{sh}} \tag{2}$$

Equation (2) takes into account particular internal physical parameters of the diode in its model. Here, V_t represents the terminal voltage, I_{sd} represents the current of the diode saturation, while R_{sh} and R_s defines the shunt and series resistance, respectively. n is the ideality factor of the diode. Some physical constants are included because of the Shockley diode equation. They include the Boltzmann constant k = $1.380 \times 10^{-23}(J/K)$, the charge magnitude of an electron $q = 1.602 \times 10^{-19}C$, and the temperature of the p-n junction of the cell (T). To accurately model the SD system, it is imperative to find the values of parameters R_{sh}, R_s, I_{ph}, I_{sd}, I_{sh}, and n that correspond to the measurable values of V_t and I_t.

Table I describes the ranges of parameters used in previous related studies [34] and are in turn, used in this thesis. These ranges are noted to not be randomly selected but are based on physical meaning to represent a feasible and realistic search space such that impractical solutions are not considered by any algorithm or solution method being employed [35, 36, 37, 38].

While the SD model is generally considered to be a good model for the SC, the literature shows that its accuracy is not sufficiently practical [39, 40, 41]. For this reason, the Double diode model is proposed.

C. Double-diode model

The Double Diode (DD) model is an integral of two diodes for different purposes - the first one is the rectifier of alternating current (AC) into direct current (DC), and the second one models recombination current loss and other semiconductor device imperfections and is called SC. That is to say that from these models, the dual-diode modification was implemented in the model described by Elias et al., and hence more accurate models have been developed taking into consideration non-ideal behaviours for low irradiation conditions for more precision in SC simulations and analysis [42, 43].

Figure 2 below shows the Double Diode (DD) arrangement depicting how two diodes can be used to recharge or control with accuracy its photo-generated current source. In this case, the arrangement is an indication of a proper design where the diodes are arranged in a row that allows for efficacy management of the current generated by the photosensitive source in the indicated arrangement.

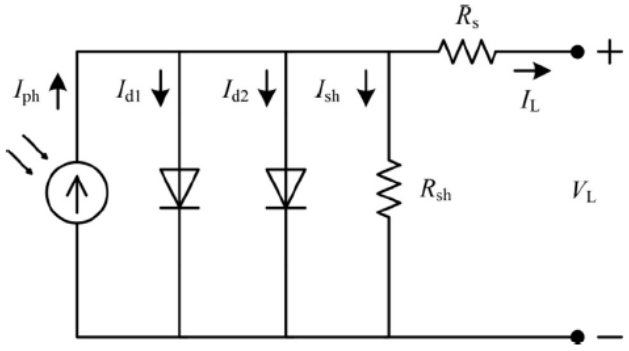

Fig. 2. A double diode circuit model

The recombination current in microdevices represents non-ideal features from a procedure where electron-hole pairs can radiate energy while they conjugate [44]. Indeed, accurate analysis and design of SC require due consideration of several non-idealities that include recombination current, leakage current, and parasitic capacitances [45]. The DD model takes into account the dual diode configuration to be more realistic in its representation and thus it contributes to greater accuracy in simulations and analysis having these non-ideal behaviours [46].

Leveraging the figure 2, (1) can be formulated as the following:

$$I_t = I_{ph} - I_{d1} - I_{d2} - I_{sh} \tag{3}$$

Where I_{d1} is the current flowing through the first diode and I_{d2} is the current flowing through the second diode. The remaining elements are specified in (1). To gain insight into the internal structure of diodes, the Shockley diode equivalence [35] is employed. Subsequently, Equation (3) transforms, resulting in the form presented in Equation (4).

$$I = I_{ph} - I_{sd1}\left[\exp\left(\frac{q(V_t + Rs \cdot I_t)}{n_1 \cdot k \cdot T}\right) - 1\right] - I_{sd2}\left[\exp\left(\frac{q(V_t + Rs \cdot I_t)}{n_2 \cdot k \cdot T}\right) - 1\right] - \frac{V_t + R_s \cdot I_t}{R_{sh}} \tag{4}$$

Here, I_{sd2} and I_{sd1} represent the saturation and diffusion currents for diode two ($d2$) and diode one ($d1$), respectively. Additionally, $n2$ and $n1$ characterize the ideality factors for the recombination and diffusion diodes, respectively. With these considerations, the DD model entails estimating seven unknown parameters: R_s, R_{sh}, I_{ph}, I_{sd1}, I_{sd2}, $n1$, and $n2$.

D. Triple-diode model

The most recent triple-diode model is described as an upgrade of the SD and DD models. It is noted for its ability to explain better and define the different current components of large-size crystalline silicon solar cells [47, 48]. It has also been shown to address issues related to recombination currents and enhance the overall performance and reliability of the system [49, 50]. The TD model is illustrated in figure 3:

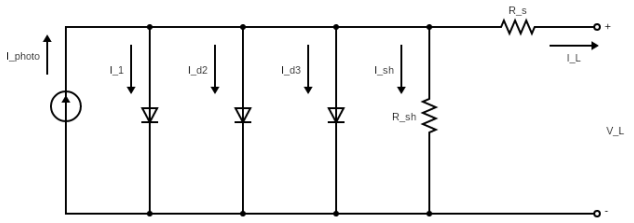

Fig. 3. A triple diode circuit model

With the addition of an extra diode, Equation (3) is then modified as:

$$I_t = I_{ph} - I_{d1} - I_{d2} - I_{d3} - I_{sh} \tag{5}$$

Applying the Shockley equivalence, Equation (5) becomes

$$I = I_{ph} - I_{sd1}\left[\exp\left(\frac{q(V_t + R_s \cdot I_t)}{n_1 \cdot k \cdot T}\right) - 1\right] - I_{sd2}\left[\exp\left(\frac{q(V_t + R_s \cdot I_t)}{n_2 \cdot k \cdot T}\right) - 1\right] \ldots - I_{sd3}\left[\exp\left(\frac{q(V_t + R_s \cdot I_t)}{n_3 \cdot k \cdot T}\right) - 1\right] - \frac{V_t + R_s \cdot I_t}{R_{sh}} \tag{6}$$

The nine parameters (R_s, R_{sh}, I_{ph}, I_{sd1}, I_{sd2}, I_{sd3}, n_1, n_2 and n_3) described by the TD model are estimated to describe the relationship between current and voltage in the SC.

III. Whale Optimization Algorithm

Humpback whales use a unique diving method to great depths, surrounding their targets in such a way that they build a spiral-shaped bubble net, then rise again during this process. They feed usually on small fish found near the surface of water bodies. This mathematical model of the hunting strategy tries to describe steps performed in the hunting i.e. how whales go around their prey, carry out the spiral bubble net manoeuvre and search for their intended target. This model can be analyzed and modelled as shown subsequently.

A. Surrounding the prey

In the application of the WOA, the prey position is the optimal solution for the entire manoeuvre. This is logically coherent as whales would opt for the position which maximises the amount of fish they can consume with one strike. The encircling dance of the whales around the prey can be represented as such [51]:

$$D = |C \cdot X_p(t) - X(t)| \tag{7}$$

$$X(t+1) = X_p(t) - A.D \tag{8}$$

where $X(t)$ is the position vector of whale position, t denotes the current iteration, $X_p(t)$ is the prey position vector, and A and C are coefficient vectors that can be computed as:

$$A = 2a \cdot r - a \tag{9}$$

$$a = 2 - 2 \cdot \left(\frac{t}{\text{iterations}_{\max}}\right) \tag{10}$$

$$C = 2 \cdot r \tag{11}$$

The vector a is linearly decreasing from two to zero with each step length depending on the ratio of the step count to the maximum number of iterations. While $r \in \text{rand}(0, 1)$ and changes with each iterative step.

B. Attacking the prey

This process includes the random combination of two states which are ultimately selected via the randomness of the variables of each iteration. In one case where $|A| < 1$ from equation (9), the whales or solution points employ equation (8) to close in on the prey (optimal solution). In another case where $|A| > 1$, the whales use a spiral behaviour to further explore the solution space. This can be computed as [51]:

$$X(t+1) = D' \cdot e^{bl} \cos(2\pi l) + X_p(t) \tag{12}$$

$$D' = |X_p(t) - X(t)| \tag{13}$$

Where b is a constant that informs the shape of the log component of the periodic function, and l is such that $l \in \text{rand}[-1, 1]$.

The solution points simultaneously leverage this surround-and-attack protocol with each iteration with an equal chance. This creates a contracting spiral path that closely resembles the behaviour of whales while hunting. The combined behaviour can be modelled as such:

$$X(t+1) = \begin{cases} X_p(t) - A \cdot D & \text{if } p < 0.5 \\ D' \cdot e^{bl} \cdot \cos(2\pi l) + X_p(t) & \text{if } p \geq 0.5 \end{cases} \quad (14)$$

C. Hunting the Prey

In reality, not all whales involved in the search may communicate effectively with the whale closest to the prey and may wander and search randomly of their own volition to find food. This necessitates the use of a coefficient A that will depict the likelihood that an individual whale follows the whale closest to the prey or attempts an individual search for the next iterative time frame. This behaviour is modelled as follows [51]:

$$D = |C \cdot X_r(t) - X(t)| \quad (15)$$

$$X(t+1) = X_r(t) - A \cdot D \quad (16)$$

where r is a random search agent. The flowchart of the WOA is illustrated in Fig 4.

D. Improved Whale Optimization Algorithm

In a paper written by Xiong et al., an improved form of the WOA (IWOA) was posited in the context of photovoltaic parameter estimation. This was because the base form of the WOA tended to get trapped in local optima due to its quick convergence at the commencement of the evolutionary phase as shown by the behaviour of the coefficient $|A|$. While this is not a problem when considering unimodal problems, it poses a problem with facing multimodal problems of which the estimation of triple diode PV systems are.

It was shown that since the coefficient $|A|$ serves to oscillate the algorithm between exploration and exploitation, the likelihood of these cases per iteration is not the same [26]. Equation (9) can be written as:

$$\begin{aligned} A &= 2a \cdot \text{rand}(0,1) - a \\ &= \left[2 \cdot \text{rand}(0,1) - 1\right] \cdot a \\ &= \gamma \cdot a \end{aligned} \quad (17)$$

where $\gamma = 2 \cdot \text{ rand } (0,1) - 1$, and is a real number which is uniformly distributed such that $\gamma \in (-1, 1)$. Now since a is linear and reducing from 2 to 0 over t iterations, it holds that $|A| = |\gamma \cdot a| < 1$ for the last half of the iterative processes as shown in fig 5.

Xiong et al. also showed that the probability of the WOA executing (8) can be expressed as:

$$\begin{aligned} P(|A| < 1) = P(|\gamma \cdot a| < 1) &= 0.5 + \int_{0.5}^{1} \int_{1}^{\frac{1}{\gamma}} \mathrm{d}a \cdot \mathrm{d}\gamma \\ &= 0.5 + \int_{0.5}^{1} \left(\frac{1}{\gamma} - 1\right) d\gamma \\ &= 0.5 + (\ln \gamma - \gamma)\Big|_{0.5}^{1} \\ &= \ln 2 \approx 0.693 \end{aligned} \quad (18)$$

This shows that in the first half of the iterative process, the whales display about a 0.7 probability of exhibiting exploratory behaviour by adjusting their direction of search based on another random search agent (who is not the closest to the prey). Including the additional probability of the search agents following a spiral path, it was shown by Xiong et al.that exploration heavily dominates the algorithm for the first half of the process. But this quickly shrinks during the second half which leaves the algorithm vulnerable to getting trapped in local minima as illustrated in figure 5. To balance exploration and exploitation, Xiong et al. proposed two additional search strategies to replace equations 16 and 8 respectively:

$$X(t+1) = X_{r_1}(t) - A \cdot |X(t) - X_{r_1}(t)| \quad (19)$$

$$X(t+1) = X_{r_1} - A \cdot |X_p(t) - X_{r_2}(t)| \quad (20)$$

where r_1 and r_2 are random search agents. Xiong et al. claimed through sufficient evidence that the use of random agents increases the diversity of the population and improves the exploration capabilities in a more balanced manner. Furthermore, the exclusion of the coefficient C reduces some randomness in the search processes but this apparent reduction in randomness is replaced by the new search strategy which guarantees a more consistently robust search.

IV. Modification Evaluation Criteria

To evaluate the efficacy of the proposed modifications, ten benchmark functions were adopted in this thesis. Six were unimodal (having one solution) and four were multimodal (having multiple solutions). The benchmark functions used in this thesis are shown in table II. To highlight the performance of the modifications from a statistical perspective, the mean and standard deviation of the last ten fitness values will be computed for each benchmark function and tabulated for clarity.

V. Exploratory Modifications

This section explores the methodology used to modify the IWOA to boost its exploratory capabilities and robustness. The modifications were tested using 10 benchmark functions, 6 of which were unimodal (having one optimum) while the remaining 4 were multi-modal with many local optima but one global optimum. The performance of the variations was illustrated by plotting the number of iterations and the

TABLE II

Name	Formula	Global Minimum	Search Domain
Sphere Function [52]	$f_1(\mathbf{x}) = \sum_{i=1}^{n} x_i^2$	0 at $\mathbf{x} = 0$	$-100 \leq x_i \leq 100$
Sum of Absolute Values [53]	$f_2(\mathbf{x}) = \sum_{i=1}^{n} \lvert x_i \rvert + \prod_{i=1}^{n} \lvert x_i \rvert$	0 at $\mathbf{x} = 0$	$-10 \leq x_i \leq 10$
Sum of Squares Function [52]	$f_3(\mathbf{x}) = \sum_{i=1}^{n} \left(\sum_{j=1}^{i} x_j \right)^2$	0 at $\mathbf{x} = 0$	$-10 \leq x_i \leq 10$
Rosenbrock Function [52, 54]	$f_5(\mathbf{x}) = \sum_{i=1}^{n-1} [100(x_{i+1} - x_i^2)^2 + (x_i - 1)^2]$	0 at $\mathbf{x} = 1$	$-2.048 \leq x_i \leq 2.048$
Step Function [55]	$f_6(\mathbf{x}) = \sum_{i=1}^{n} (x_i + 0.5)^2$	0 at $\mathbf{x} = -0.5$	$-100 \leq x_i \leq 100$
Quartic Function [55]	$f_7(\mathbf{x}) = \sum_{i=1}^{n} i \cdot x_i^4 + \text{random}[0, 1]$	0 at $\mathbf{x} = 0$	$-1.28 \leq x_i \leq 1.28$
Schwefel Function [52]	$f_8(\mathbf{x}) = \sum_{i=1}^{n} -x_i \sin(\sqrt{\lvert x_i \rvert})$	$418.9829n$ at $\mathbf{x} = 420.9687$	$-500 \leq x_i \leq 500$
Rastrigin Function [52, 56]	$f_9(\mathbf{x}) = \sum_{i=1}^{n} [x_i^2 - 10\cos(2\pi x_i) + 10]$	0 at $\mathbf{x} = 0$	$-5.12 \leq x_i \leq 5.12$
Ackley Function [52, 57, 58]	$f_{10}(\mathbf{x}) = -20\exp\left(-0.2\sqrt{\frac{1}{n}\sum_{i=1}^{n} x_i^2}\right)$ $-\exp\left(\frac{1}{n}\sum_{i=1}^{n}\cos(2\pi x_i)\right) + 20 + e$	0 at $\mathbf{x} = 0$	$-32 \leq x_i \leq 32$
Griewank Function [52]	$f_{11}(\mathbf{x}) = \frac{1}{4000}\sum_{i=1}^{n} x_i^2 - \prod_{i=1}^{n} \cos\left(\frac{x_i}{\sqrt{i}}\right) + 1$	0 at $\mathbf{x} = 0$	$-600 \leq x_i \leq 600$

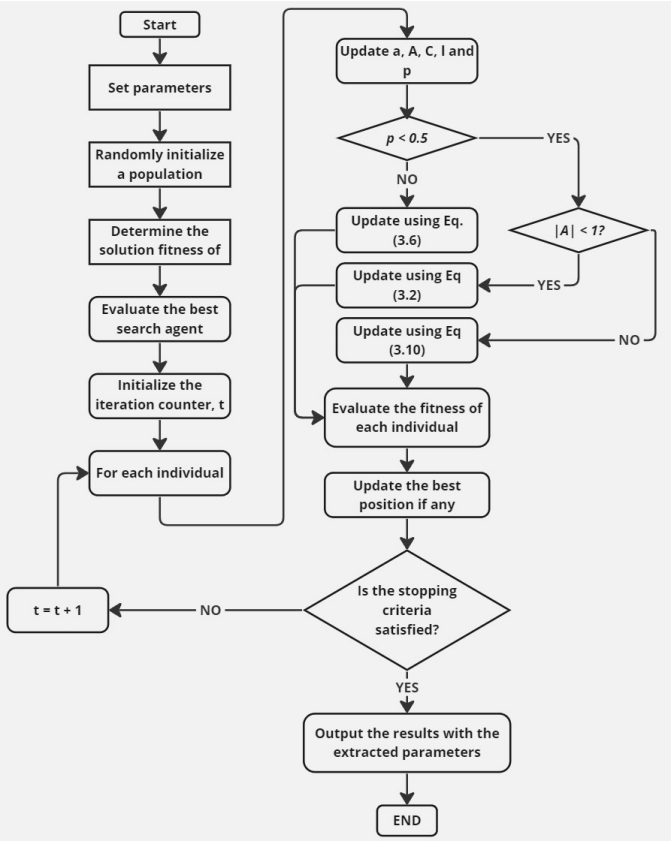

Fig. 4. The WOA flowchart

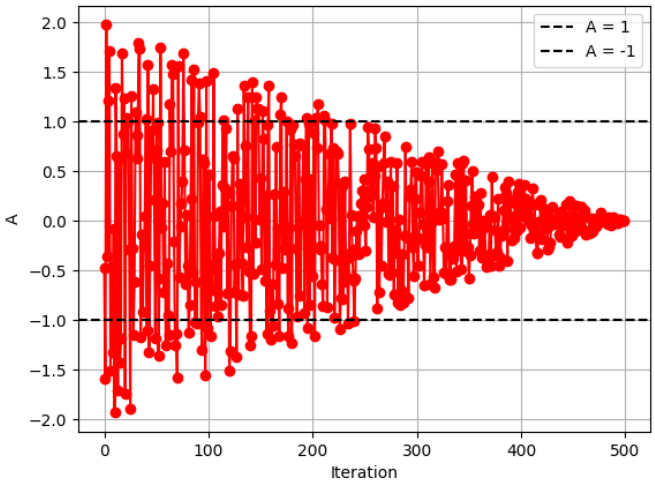

Fig. 5. Distribution of A for linearly decreasing values of a

fitness value for 10 distinct experiments, for each benchmark function. Furthermore, a statistical overview was done to comprehensively analyse the means and standard deviation of the last fitness values of the 10 experiments for each benchmark function. The best-performing exploratory modification will be selected and applied to the research case of estimating the parameters of the triple-diode PV system.

As highlighted, the value of $|A|$ serves as a metric that leads the algorithm to either exploration or exploitation after the value of p has been randomized for the current iterative step. This infers that the manipulation of the properties of the component variable 'a' can in turn adjust the distribution spread or likelihood of $|A|$ values which fall below or above 1.

To improve the robustness and exploratory capability of the IWOA even further, the following functions in the next few subsections were considered in replacement of equation (10).

These modifications to the IWOA were tested using unimodal and multimodal benchmark functions [52] as shown in table III to VI. Experiments were performed and graphed for each modification, across the 10 different benchmark functions. All benchmark tests and experiments were carried out on a 3.3-GHz AMD Ryzen 5 5600H Radeon processor (12 CPUs) with 16.0 GB RAM using Python 3.11.2.

A. Sinusoidal variation

This variation of a adopts the sine function to introduce periodicity in the randomly converging spread of the values of A.

$$a = 2 + \sin\left(\frac{2\pi i}{\max_{\text{iter}}}\right) \tag{21}$$

Where i is the ith iteration in the range of maximum epochs. This variation ensures that the algorithm maintains a more exploratory stance even after the first half of the total iterations as shown in figure 6. For the sample experiment displayed, of the 500 epochs, a total of 225 iterations of $|A|$ lay above 1 while the remaining 275 were below which is a more balanced distribution compared with the classic case. The function allows for some exploratory behaviour towards the end of the search. This gives room for the algorithm to be more likely to escape possible local minima. Convergence was rather quick for the unimodal functions apart from the quartic function due to noise. Regardless of the unimodality of the other functions, a few delays in convergence were detected as a result of the increased exploratory predisposition of the modified algorithm. This means that in the unimodal case where there exists just one solution, the algorithm will still prefer to "look around" just to make sure. And this extra space search causes some delays in convergence speed. While not generally ideal, for the thesis objective of increased robustness, this serves our eventual needs.

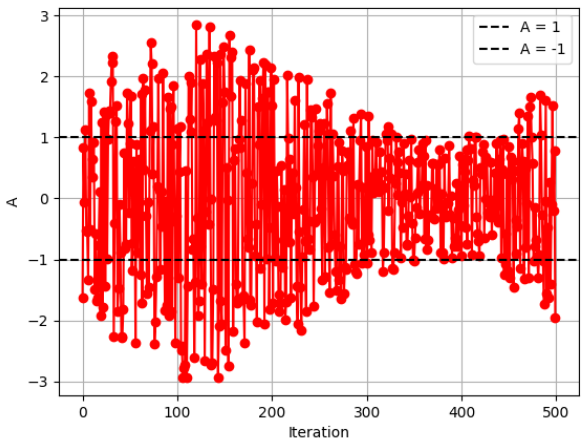

Fig. 6. The distribution of A for the sinusoidal variation of a

As for the multimodal functions, the modifications assisted the algorithm to escape the local minima in two separate experiments in the Schwefel function after less than 18 iterations. This will take longer in a case where the IWOA did not have a sufficiently higher exploratory likelihood. One experiment was observed to plateau for a little under 20 iterations before escaping the local minimum and converging to the global optimum like the rest.

A statistical analysis was executed on the last fitness of each experiment to ascertain the average performance of the modification, as well as the standard deviation of these last fitness values, across all benchmark tests. The table III shows the results, including all the necessary details to make the modification performance more comprehensive. The variation allowed the modified IWOA to perform quite well against all but the Rastrigin function which had a high mean of 2.756×10^{-1} even after 500 iterations.

B. Oscillatory variation

A periodic function can be used to either increase or decrease the distribution likelihood of points of A which lie above or below 1 for every iteration. The equation for this variation is given by:

$$a = 1.5 + \sin\left(i \cdot \frac{\pi}{\max_{\text{iter}}}\right) \tag{22}$$

In such cases, we define all possible behaviours to be distributed across half the cycle of a sine function as $\frac{i}{\max_{\text{iter}}}$ approaches 1 for any maximum number of iterations. The behaviour for a random experiment is shown in figure 7. For a typical random experiment with 500 iterations, 265 points lay outside the $A(-1, 1)$ interval, while the remaining 235 lay within. Compared to the classic linearly decreasing a, this modification ensures that $|A|$ maintains a more even spread of exploration and exploitation likelihood throughout the entire evolutionary phase. The variation shows a quickly convergent behaviour on unimodal functions with the longest taking a little under 20 iterations to converge. Unlike the sinusoidal variation, this variation handled the quartic function quite well with only one experiment converging past 40 iterations due to noise.

The statistical overview of the performance of the oscillatory variation of the IWOA is shown in table IV. Across the unimodal functions, the variation performed best on the sum of squares function with a mean convergence of 1.53×10^{-9} across 10 experiments.

C. Inverse Relationship

This modification leverages an inverse function that provides a high likelihood at the beginning which slowly decreases as more iterations are carried out. By adjusting the coefficients of the function, we're able to make sure that there exist more points of A such that $A \notin (-1, 1)$. This improves the algorithm's robustness as the search algorithm's stance becomes more exploratory above the first half of the evolutionary phase as shown in figure 8. The equation for this modified parameter a is given by:

TABLE III
THE SINUSOIDAL VARIATION'S PERFORMANCE ON BENCHMARK FUNCTIONS

Function	Domain range	Global Minimum	Epochs	Dimension	Mean of last fitness	Std. dev. of last fitness
Sphere	(-100, 100)	0	500	2	1.0547×10^{-3}	1.4372×10^{-3}
Sum of absolute values	(-10,10)	0	500	2	1.1345×10^{-3}	1.0334×10^{-3}
Sum of squares	(-10, 10)	0	500	2	6.08×10^{-10}	7.05×10^{-10}
Rosenbrock	(-2.048, -2.048)	0	500	2	1.15398×10^{-4}	2.6038×10^{-4}
Step	(-100, 100)	0	500	2	2.7083×10^{-4}	3.1478×10^{-4}
Quartic (with noise)	(-1.28,1.28)	0	500	9	5.54498×10^{-2}	3.8289×10^{-2}
Schwefel	(-500, 500)	418.9829	500	1	4.189829×10^{2}	3.99×10^{-6}
Rastrigin	(-5.12, 5.12)	0	500	2	2.7568×10^{-1}	4.2866×10^{-1}
Ackley	(-32, 32)	0	500	2	1.5969×10^{-2}	8.6136×10^{-3}
Griewank	(-600, 600)	0	500	2	4.1652×10^{-2}	3.4596×10^{-2}

TABLE IV
THE OSCILLATORY VARIATION'S PERFORMANCE ON BENCHMARK FUNCTIONS

Function	Domain range	Global Minimum	Epochs	Dimension	Mean of last fitness	Std. dev. of last fitness
Sphere	(-100, 100)	0	500	2	6.4987×10^{-4}	7.3814×10^{-4}
Sum of absolute values	(-10, 10)	0	500	2	1.4544×10^{-3}	1.0189×10^{-3}
Sum of squares	(-10, 10)	0	500	2	1.53×10^{-9}	1.47×10^{-9}
Rosenbrock	(-2.048, 2.048)	0	500	2	2.1202×10^{-4}	5.0749×10^{-4}
Step	(-100, 100)	0	500	2	2.6646×10^{-4}	2.1807×10^{-4}
Quartic (with noise)	(-1.28, 1.28)	0	500	9	7.8877×10^{-2}	7.8642×10^{-2}
Schwefel	(-500, 500)	418.9829	500	1	4.1898×10^{2}	7.20×10^{-7}
Rastrigin	(-5.12, 5.12)	0	500	2	1.4185×10^{-2}	2.8252×10^{-2}
Ackley	(-32, 32)	0	500	2	2.6838×10^{-2}	1.6937×10^{-2}
Griewank	(-600, 600)	0	500	2	4.0244×10^{-2}	4.4035×10^{-2}

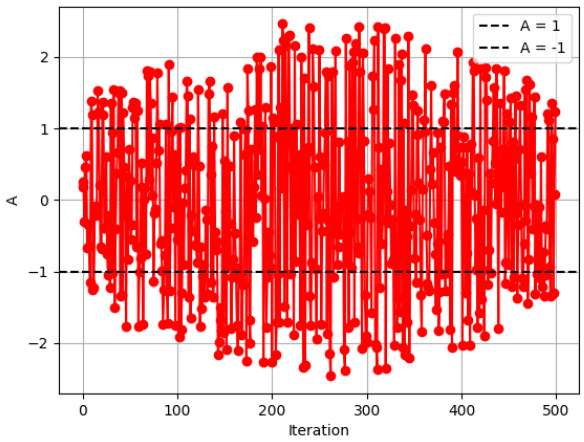

Fig. 7. The distribution of A for the oscillatory variation of a

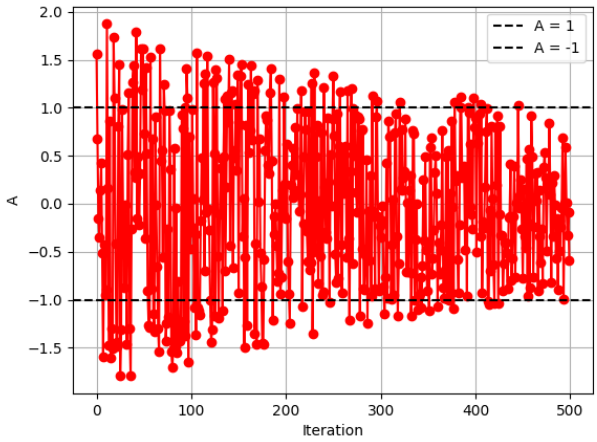

Fig. 8. The distribution of A for the inverse variation of a

$$a = 2 \cdot \left(1 + \frac{i}{\max_{\text{iter}}}\right)^{-1} \tag{23}$$

The modification was seen to pass the uni-modal and multi-modal functions that they were given. Convergence occurred quickly on the uni-modal functions, with the latest convergence occurring at the 60th iteration for the sum of absolutes functions.

As for the multi-modal functions in figure 8, the modification was able to break out of local minima quite reliably, with the longest time being stuck, which was for a bit over 50 iterations for the Ackley function. With a sufficient amount of exploratory likelihood, the scheme showed a decent ability to escape local minima given an extended number of iterations. Table V shows the statistical overview of the performance of the inverse variation. The modification performed decently across the board with the weakest performance being on the

Quartic and Griewank functions.

D. Exponential decrease

This modification on a uses a nonlinear decrease in the form of an exponential decay to guide the spread of the output of A. Similar to the inverse modification, we attempt to have more guided control of the amount of A values below 1, per iteration. The equation for this relation is as follows:

$$a = 2.5 \cdot \exp\left(\frac{-i}{\max_{\text{iter}} - 1}\right) \tag{24}$$

Using the coefficient of the exponential function, we can adjust the amplitude of the distribution of A values to ensure some more exploration-guided iterations, even after the middle mark. A random experiment revealed that for 500 maximum iterations for $|A|$, a total of 162 points were above 1 while the remaining 338 lay below 1 as illustrated in figure 9.

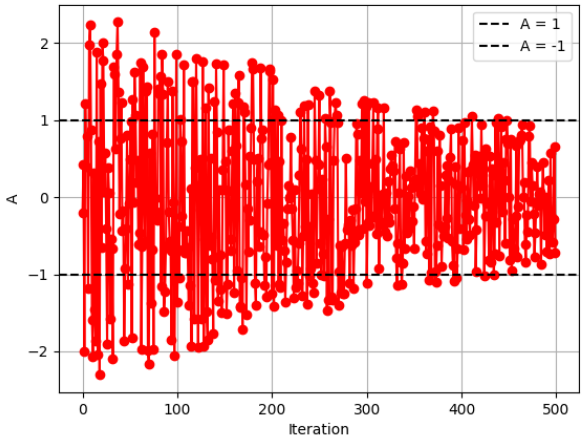

Fig. 9. The distribution of A for the exponential decrease of a

This will imply a greater likelihood of search agents subscribing to a more exploratory stance, than the classic case. The graphical performance showed that the modification was able to converge to the global minima on the benchmark tests given to it. The modification's ability to break out of local minima was verified. The statistical overview of the modification is shown in table VI.

VI. Exploitation Modifications

This section explores two methodologies that can be potentially used to modify and rudder the IWOA for more exploitation in a contained manner. As in the exploratory cases above, these modifications were plotted so that their behaviour and spread of likelihood are comprehensible, and their performances were tested using the same benchmark functions above. Statistical analysis was again performed on the last fitness generated by each of the 10 experiments and the insights were recorded and shown from table VII and VIII.

A. Quadratic Decrease

This modification leverages a non-linear decreasing behaviour of a by using a special quadratic decay as shown in equation 25. By setting the constant to 0.14, we can ensure that out of the 500 iterations, values of $|A|$ from the 200th iteration and upwards will be strictly less than 1. This ensures an even quicker convergence to minima which may be useful in unimodal cases to reduce computation resources.

$$a = \left(\frac{14}{100} - \frac{i}{\max_{\text{iter}} - 1}\right)^2 \tag{25}$$

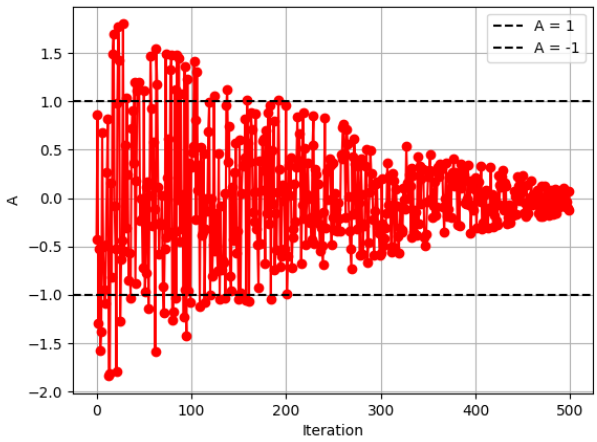

Fig. 10. The distribution of A for the quadratic decrease of a

For this modification, a random experiment with 500 iterations showed that $|A| < 1$ for 444 instances, while $|A| > 1$ for the remaining 56 as shown in figure 10. In terms of solution quality, the modification showed a slightly weaker performance on the benchmark functions, evidenced by a higher chance of getting stuck in local minima for a few unimodal functions. As expected, convergence was quick in most cases, with the longest benchmark taking 40 iterations to converge. Due to the higher exploitation bias, the modification performed considerably weaker for the quartic function (with noise) where only one of the 10 experiments converged to near-zero. As for the other multimodal functions, the modification still managed to escape local minima but this is solely a result of the efficacy of the IWOA and its improved search strategy. Nevertheless, the increased exploitation likelihood can still be seen, compared with other exploratory modifications. The statistical performance is shown in table VII.

B. Logarithmic Variation

For this variation, we adopt the log function shown in Equation 26 as a non-linear way to decrease the parameter a as the iterations proceed. Initially, the log term will always equal to 0 for any positive number of iterations ($\max_{\text{iter}} > 1$), such that $a = 2$ at first.

TABLE V
THE INVERSE VARIATION'S PERFORMANCE ON BENCHMARK FUNCTIONS

Function	Domain range	Global Minimum	Epochs	Dimension	Mean of last fitness	Std. dev. of last fitness
Sphere	(-100, 100)	0	500	2	6.4420×10^{-4}	1.2359×10^{-3}
Sum of absolute values	(-10, 10)	0	500	2	1.3076×10^{-3}	1.0470×10^{-3}
Sum of squares	(-10, 10)	0	500	2	4.73×10^{-10}	4.53×10^{-10}
Rosenbrock	(-2.048, 2.048)	0	500	2	9.24×10^{-6}	1.97×10^{-5}
Step	(-100, 100)	0	500	2	2.0034×10^{-3}	3.4020×10^{-3}
Quartic (with noise)	(-1.28, 1.28)	0	500	9	6.3643×10^{-2}	3.6556×10^{-2}
Schwefel	(-500, 500)	418.9829	500	1	4.1898×10^{2}	1.42×10^{-6}
Rastrigin	(-5.12, 5.12)	0	500	2	3.2107×10^{-4}	4.9108×10^{-4}
Ackley	(-32, 32)	0	500	2	1.8405×10^{-2}	2.0925×10^{-2}
Griewank	(-600, 600)	0	500	2	4.7828×10^{-2}	4.5765×10^{-2}

TABLE VI
THE EXPONENTIAL VARIATION'S PERFORMANCE ON BENCHMARK FUNCTIONS

Function	Domain range	Global Minimum	Epochs	Dimension	Mean of last fitness	Std. dev. of last fitness
Sphere	(-100, 100)	0	500	2	1.1836×10^{-3}	2.3092×10^{-3}
Sum of absolute values	(-10, 10)	0	500	2	2.3663×10^{-3}	3.4024×10^{-3}
Sum of squares	(-10, 10)	0	500	2	9.20×10^{-10}	1.66×10^{-9}
Rosenbrock	(-2.048, 2.048)	0	500	2	6.42×10^{-5}	1.7681×10^{-4}
Step	(-100, 100)	0	500	2	2.8941×10^{-4}	1.8834×10^{-4}
Quartic (with noise)	(-1.28, 1.28)	0	500	9	4.1799×10^{-2}	2.4264×10^{-2}
Schwefel	(-500, 500)	418.9829	500	1	4.1898×10^{2}	7.74×10^{-7}
Rastrigin	(-5.12, 5.12)	0	500	2	2.9937×10^{-1}	4.5702×10^{-1}
Ackley	(-32, 32)	0	500	2	1.5656×10^{-2}	1.0228×10^{-2}
Griewank	(-600, 600)	0	500	2	5.5895×10^{-2}	3.8900×10^{-2}

TABLE VII
THE QUADRATICALLY DECREASING VARIATION'S PERFORMANCE ON BENCHMARK FUNCTIONS

Function	Domain range	Global Minimum	Epochs	Dimension	Mean of last fitness	Std. dev. of last fitness
Sphere	(-100, 100)	0	500	2	4.9452×10^{-4}	5.8251×10^{-4}
Sum of absolute values	(-10, 10)	0	500	2	9.8680×10^{-4}	1.1593×10^{-3}
Sum of squares	(-10, 10)	0	500	2	8.32×10^{-10}	1.54×10^{-9}
Rosenbrock	(-2.048, 2.048)	0	500	2	7.13×10^{-5}	1.0248×10^{-4}
Step	(-100, 100)	0	500	2	1.8734×10^{-3}	3.8821×10^{-3}
Quartic (with noise)	(-1.28, 1.28)	0	500	9	6.0907×10^{-2}	6.8556×10^{-2}
Schwefel	(-500, 500)	418.9829	500	1	4.1898×10^{2}	1.41×10^{-6}
Rastrigin	(-5.12, 5.12)	0	500	2	7.1003×10^{-4}	1.5587×10^{-3}
Ackley	(-32, 32)	0	500	2	1.5653×10^{-2}	1.3175×10^{-2}
Griewank	(-600, 600)	0	500	2	3.2023×10^{-2}	2.8009×10^{-2}

$$a = 2 - \log_{\max_{\text{iter}}}(i+1) \tag{26}$$

Apart from the non-linear and stepwise manner in which the log function generally decelerates, it's important to note that the 'base' of the logarithmic function (which is the maximum number of iterations in this case) is a key setting that will slow down the pace at which a descends. This is because the higher the base ($\max_{\text{iter}}$) is, the slower the pace at which a descends will be. This holds as more significant changes in i will be needed to cause the same amount of change in a.

As shown in figure 11, for 500 iterations of $|A|$, 67 points lay above 1, while the remaining 433 lay below 1. This demonstrates a higher propensity towards exploitation by the algorithm with this modification. Moreover, it can be seen that for the first 20% of iterations, more of the points where $|A|$ is above 1, are concentrated. This is a result of the logarithmic property of a.

The benchmark tests on the log variation revealed a more sluggish convergence speed towards the global minimum. This is expected due to the high exploitation likelihood of the algorithm as a result of the modification. The algorithm was noticed to use two or three iterations to move past a current fitness or position when dealing with unimodal benchmarks. This effect was greatly increased when handling multimodal benchmark solutions such as the Schwefel and Ackley functions. While eventual convergence did occur, the noted inefficiency of this modification may create additional computation requirements when applied to various practical problems. The logarithmic variation may not be the most

TABLE VIII
THE LOGARITHMIC VARIATION'S PERFORMANCE ON BENCHMARK FUNCTIONS

Function	Domain range	Global Minimum	Epochs	Dimension	Mean of last fitness	Std. dev. of last fitness
Sphere	(-100, 100)	0	500	2	2.3071×10^{-4}	2.6457×10^{-4}
Sum of absolute values	(-10, 10)	0	500	2	1.1128×10^{-3}	1.0178×10^{-3}
Sum of squares	(-10, 10)	0	500	2	9.91×10^{-10}	1.12×10^{-9}
Rosenbrock	(-2.048, 2.048)	0	500	2	5.68×10^{-5}	1.0487×10^{-4}
Step	(-100, 100)	0	500	2	4.7594×10^{-4}	7.0928×10^{-4}
Quartic (with noise)	(-1.28, 1.28)	0	500	9	3.7805×10^{-2}	1.2056×10^{-2}
Schwefel	(-500, 500)	418.9829	500	1	4.1898×10^{2}	6.48×10^{-7}
Rastrigin	(-5.12, 5.12)	0	500	2	6.8722×10^{-4}	1.6527×10^{-3}
Ackley	(-32, 32)	0	500	2	1.2142×10^{-2}	1.0360×10^{-2}
Griewank	(-600, 600)	0	500	2	4.4344×10^{-2}	3.7551×10^{-2}

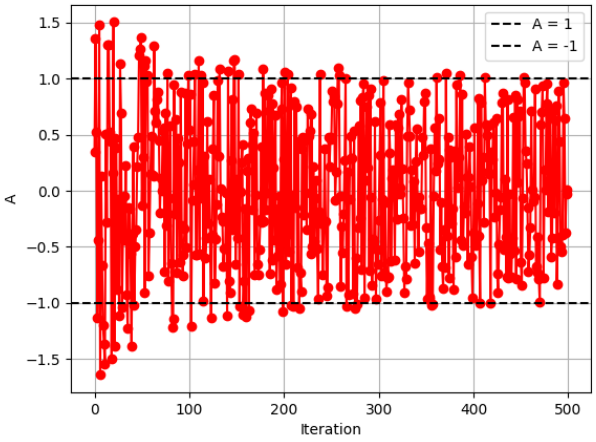

Fig. 11. The distribution of A for the logarithmic decrease of a

effective exploitation modification for cases with a maximum iteration count too high. Table VIII highlights the statistical performance of the modification.

VII. Evaluation Criteria

To extract the parameters from the previously discussed PV models from the I-V dataset, whatever optimization technique is being used needs a function to define the objective of the system before it discovers a way to optimize it properly. In previous studies, the root-mean-square error [59] is vastly engaged to describe the objective function by showing how far off the estimated values of the current is, from what has been recorded or measured.

This error is the algorithm's fitness function and is described as follows:

$$\textbf{min}F(x) = \textbf{RMSE}(x) = \sqrt{\frac{1}{N_E} \cdot \sum_{i=1}^{N_E} f_x(V_t, I_t, \Phi)^2} \quad (27)$$

where N_E is the number of samples of experimental data, and Φ is the decision vector of the parameters to be computed. For the research case which will be on the triple diode model, Φ will be the vector-array (R_s, R_{sh}, I_{ph}, I_{sd1}, I_{sd2}, I_{sd3}, n_1, n_2 and n_3). The modifications will be employed to minimize this function.

VIII. Results

The final procedure involved taking a sample measurement from the experimental methods described in Table 4 from the paper on the IWOA by Khanna et al. [47]. The idea was to attempt to replicate the experiment, using all the data variables from the previous research as pseudo-control variables such that the effect of the modifications can be examined more comparatively. The final application was attempted using Python 3.11.2 [60] on the same system specifications disclosed above in the section on Exploratory Modification.

In an attempt to generate an I-V curve using the data sample, a range of continuous voltage values was first defined which spanned from 0 volts to a value just beyond the open-circuit voltage of the module being modelled. Next, a 'triple-diode-model' function modelled after equation 6 was defined using Python's Scipy library [61] and used to calculate the corresponding current (I) based on the set of data variables collected from Khanna et al.'s research. The same variable bounds for each of the parameters were declared as a list of tuples with each tuple containing the bounds of each variable to be estimated. The temperature was set to STC at 330 degrees Kelvin. The final step was for the set of current values and the matplotlib python library [62] to be used to plot and generate the I-V curve which the modified IWOA will attempt to calculate. Unfortunately, this led to unforeseen limitations which were not resolvable given the research time frame and hence did not allow the final experimental phase of the thesis to be executed. However, pre-experiment results show a good possibility of improved parameter estimation for triple-diode models and a way to measurably tune the bias of the algorithm. The online repository for these methods has been referenced in this thesis [63].

IX. Conclusions and Future Work

In this thesis, six modifications to the coefficient A in the improved whale algorithm were proposed to improve its parameter extraction performance. Two of the six modifications leveraged algebraic functions while the remaining four adopted

transcendental functions. The functions were plotted and tested using ten benchmark functions. The modifications were shown to sustain the feasibility of the algorithm as an optimizer while providing measurable adjustments to the algorithm's exploration-exploitation balance. In future work, the effect of the modifications to the parameter estimation of triple-diode photovoltaic models will be empirically investigated in full.

References

[1] J. Kaldellis, G. Spyropoulos, K. Kavadias, and I. Koronaki, "Experimental validation of autonomous pv-based water pumping system optimum sizing," *Renewable Energy*, vol. 34, no. 4, pp. 1106–1113, 2009.

[2] L. C. Ding, A. Akbarzadeh, and L. Tan, "A review of power generation with thermoelectric system and its alternative with solar ponds," *Renewable and sustainable energy reviews*, vol. 81, pp. 799–812, 2018.

[3] A. H. Elsheikh, S. W. Sharshir, M. K. A. Ali, J. Shaibo, E. M. Edreis, T. Abdelhamid, C. Du, and Z. Haiou, "Thin film technology for solar steam generation: A new dawn," *Solar Energy*, vol. 177, pp. 561–575, 2019.

[4] I. Purohit and P. Purohit, "Technical and economic potential of concentrating solar thermal power generation in india," *Renewable and Sustainable Energy Reviews*, vol. 78, pp. 648–667, 2017.

[5] W. Charfi, M. Chaabane, H. Mhiri, and P. Bournot, "Performance evaluation of a solar photovoltaic system," *Energy Reports*, vol. 4, pp. 400–406, 2018.

[6] B. Yang, J. Wang, X. Zhang, T. Yu, W. Yao, H. Shu, F. Zeng, and L. Sun, "Comprehensive overview of meta-heuristic algorithm applications on pv cell parameter identification," *Energy Conversion and Management*, vol. 208, p. 112595, 2020.

[7] H. Rezk and M. Abdelkareem, "Optimal parameter identification of triple diode model for solar photovoltaic panel and cells," *Energy Reports*, vol. 8, 11 2021.

[8] S. Akhil, S. Akash, A. Pasha, B. Kulkarni, M. Jalalah, M. Alsaiari, F. A. Harraz, and R. G. Balakrishna, "Review on perovskite silicon tandem solar cells: Status and prospects 2t, 3t and 4t for real world conditions," *Materials & Design*, vol. 211, p. 110138, 2021.

[9] T. Bäck and H.-P. Schwefel, "An overview of evolutionary algorithms for parameter optimization," *Evolutionary Computation*, vol. 1, no. 1, pp. 1–23, 1993.

[10] P. A. Vikhar, "Evolutionary algorithms: A critical review and its future prospects," in *2016 International Conference on Global Trends in Signal Processing, Information Computing and Communication (ICGTSPICC)*, 2016, pp. 261–265.

[11] S. Gao, K. Wang, S. Tao, T. Jin, H. Dai, and J. Cheng, "A state-of-the-art differential evolution algorithm for parameter estimation of solar photovoltaic models," *Energy Conversion and Management*, vol. 230, p. 113784, 2021.

[12] J. D. Bastidas-Rodriguez, G. Petrone, C. A. Ramos-Paja, and G. Spagnuolo, "A genetic algorithm for identifying the single diode model parameters of a photovoltaic panel," *Mathematics and Computers in Simulation*, vol. 131, pp. 38–54, 2017.

[13] B. Hajek, "A tutorial survey of theory and applications of simulated annealing," in *1985 24th IEEE Conference on Decision and Control*. IEEE, 1985, pp. 755–760.

[14] R. B. Messaoud, "Extraction of uncertain parameters of double-diode model of a photovoltaic panel using simulated annealing optimization," *The Journal of Physical Chemistry C*, 2019. [Online]. Available: https://api.semanticscholar.org/CorpusID:209711488

[15] X.-S. Yang, M. Karamanoglu, and X. He, "Flower pollination algorithm: a novel approach for multiobjective optimization," *Engineering optimization*, vol. 46, no. 9, pp. 1222–1237, 2014.

[16] C. C, Taha, M. Shaji, R. R. Y, M. Jawwad, and G. Sharma, "A novel optimization method for parameter extraction of industrial solar cells," *2019 Innovations in Power and Advanced Computing Technologies (i-PACT)*, vol. 1, pp. 1–6, 2019. [Online]. Available: https://api.semanticscholar.org/CorpusID:210697813

[17] D. Wang, D. Tan, and L. Liu, "Particle swarm optimization algorithm: an overview," *Soft computing*, vol. 22, pp. 387–408, 2018.

[18] V. Khanna, B. K. Das, D. C. S. Bisht, Vandana, and P. K. Singh, "Estimation of photovoltaic cells model parameters using particle swarm optimization," 2014. [Online]. Available: https://api.semanticscholar.org/CorpusID:117185206

[19] S. A. E. Mohamed, H. M. A. Mageed, W. A. Ahmed, and A. A. Saleh, "Estimate the parameters of photovoltaic module by fodpso," *International journal of engineering research and technology*, vol. 9, 2020. [Online]. Available: https://api.semanticscholar.org/CorpusID:221567068

[20] L. Guo, Z. Meng, Y. Sun, and L. Wang, "Parameter identification and sensitivity analysis of solar cell models with cat swarm optimization algorithm," *Energy Conversion and Management*, vol. 108, pp. 520–528, 2016. [Online]. Available: https://api.semanticscholar.org/CorpusID:110591973

[21] N. Rana, M. S. A. Latiff, S. M. Abdulhamid, and H. Chiroma, "Whale optimization algorithm: a systematic review of contemporary applications, modifications and developments," *Neural Computing and Applications*, vol. 32, pp. 16 245–16 277, 2020.

[22] D. Yousri, H. Rezk, and A. Fathy, "Identifying the parameters of different configurations of photovoltaic models based on recent artificial ecosystem-based optimization approach," *International Journal of Energy Research*, vol. 44, no. 14, pp. 11 302–11 322, 2020.

[23] S. T. Kebir, M. S. A. Cheikh, and M. Haddadi, "A set of smart swarm-based optimization algorithms applied for determining solar photovoltaic cell's parameters," *Renewable Energy for Smart and Sustainable Cities*, 2018. [Online]. Available: https://api.semanticscholar.org/CorpusID:69716100

[24] C. S. Kumar and R. S. Rao, "A novel global mpp tracking of photovoltaic system based on whale optimization algorithm," *International Journal of Renewable Energy Development*, vol. 5, no. 3, pp. 225–232, 2016.

[25] J. Luo and B. Shi, "A hybrid whale optimization algorithm based on modified differential evolution for global optimization problems," *Applied Intelligence*, vol. 49, pp. 1982–2000, 2019.

[26] G. Xiong, J. Zhang, D. Shi, and Y. He, "Parameter extraction of solar photovoltaic models using an improved whale optimization algorithm," *Energy conversion and management*, vol. 174, pp. 388–405, 2018.

[27] J. Charles, M. Abdelkrim, Y. Muoy, and P. Mialhe, "A practical method of analysis of the current-voltage characteristics of solar cells," *Solar cells*, vol. 4, no. 2, pp. 169–178, 1981.

[28] D. Fuchs and H. Sigmund, "Analysis of the current-voltage characteristic of solar cells," *Solid-state electronics*, vol. 29, no. 8, pp. 791–795, 1986.

[29] V. Quaschning and R. Hanitsch, "Numerical simulation of current-voltage characteristics of photovoltaic systems with shaded solar cells," *Solar energy*, vol. 56, no. 6, pp. 513–520, 1996.

[30] M. Azzouzi, D. Popescu, and M. Bouchahdane, "Modeling of electrical characteristics of photovoltaic cell considering single-diode model," *Journal of Clean Energy Technologies*, vol. 4, no. 6, pp. 414–420, 2016.

[31] T. Ahmad, S. Sobhan, and M. F. Nayan, "Comparative analysis between single diode and double diode model of pv cell: concentrate different parameters effect on its efficiency," *Journal of power and Energy Engineering*, vol. 4, no. 3, pp. 31–46, 2016.

[32] V. Khanna, B. Das, D. Bisht, P. Singh *et al.*, "A three diode model for industrial solar cells and estimation of solar cell parameters using pso algorithm," *Renewable Energy*, vol. 78, pp. 105–113, 2015.

[33] G. Ciulla, V. L. Brano, V. Di Dio, and G. Cipriani, "A comparison of different one-diode models for the representation of i–v characteristic of a pv cell," *Renewable and Sustainable Energy Reviews*, vol. 32, pp. 684–696, 2014.

[34] T. Easwarakhanthan, J. Bottin, I. Bouhouch, and C. Boutrit, "Nonlinear minimization algorithm for determining the solar cell parameters with microcomputers," *International journal of solar energy*, vol. 4, no. 1, pp. 1–12, 1986.

[35] D. Oliva, M. Abd Elaziz, A. H. Elsheikh, and A. A. Ewees, "A review on meta-heuristics methods for estimating parameters of solar cells," *Journal of Power Sources*, vol. 435, p. 126683, 2019.

[36] A. Laudani, F. R. Fulginei, and A. Salvini, "High performing extraction procedure for the one-diode model of a photovoltaic panel from experimental i–v curves by using reduced forms," *Solar Energy*, vol. 103, pp. 316–326, 2014.

[37] Q. Niu, L. Zhang, and K. Li, "A biogeography-based optimization algorithm with mutation strategies for model parameter estimation of solar and fuel cells," *Energy conversion and management*, vol. 86, pp. 1173–1185, 2014.

[38] A. Jain and A. Kapoor, "Exact analytical solutions of the parameters of real solar cells using lambert w-function," *Solar Energy Materials and Solar Cells*, vol. 81, no. 2, pp. 269–277, 2004.

[39] B. Parida, S. Iniyan, and R. Goic, "A review of solar photovoltaic technologies," *Renewable and sustainable energy reviews*, vol. 15, no. 3, pp. 1625–1636, 2011.

[40] N. J. Sheikh, D. F. Kocaoglu, and L. Lutzenhiser, "Social and political impacts of renewable energy: Literature review," *Technological Forecasting and Social Change*, vol. 108, pp. 102–110, 2016.

[41] R. Rajesh and M. C. Mabel, "A comprehensive review of photovoltaic systems," *Renewable and sustainable energy reviews*, vol. 51, pp. 231–248, 2015.

[42] J. Gow and C. Manning, "Development of a photovoltaic array model for use in power-electronics simulation studies," *IEE Proceedings-Electric Power Applications*, vol. 146, no. 2, pp. 193–200, 1999.

[43] S. Gupta, H. Tiwari, M. Fozdar, and V. Chandna, "Development of a two diode model for photovoltaic modules suitable for use in simulation studies," in *2012 Asia-Pacific Power and Energy Engineering Conference*. IEEE, 2012, pp. 1–4.

[44] K. Ramspeck, K. Bothe, D. Hinken, B. Fischer, J. Schmidt, and R. Brendel, "Recombination current and series resistance imaging of solar cells by combined luminescence and lock-in thermography," *Applied Physics Letters*, vol. 90, no. 15, 2007.

[45] K. Tvingstedt, L. Gil-Escrig, C. Momblona, P. Rieder, D. Kiermasch, M. Sessolo, A. Baumann, H. J. Bolink, and V. Dyakonov, "Removing leakage and surface recombination in planar perovskite solar cells," *ACS Energy Letters*, vol. 2, no. 2, pp. 424–430, 2017.

[46] M. Saad and A. Kassis, "Effect of interface recombination on solar cell parameters," *Solar energy materials and solar cells*, vol. 79, no. 4, pp. 507–517, 2003.

[47] V. Khanna, B. Das, D. Bisht, P. Singh *et al.*, "A three diode model for industrial solar cells and estimation of solar cell parameters using pso algorithm," *Renewable Energy*, vol. 78, pp. 105–113, 2015.

[48] M. A. Mughal, Q. Ma, and C. Xiao, "Photovoltaic cell parameter estimation using hybrid particle swarm optimization and simulated annealing," *Energies*, vol. 10, no. 8, p. 1213, 2017.

[49] O. S. Elazab, H. M. Hasanien, M. A. Elgendy, and A. M. Abdeen, "Parameters estimation of single-and multiple-diode photovoltaic model using whale optimisation algorithm," *IET Renewable Power Generation*, vol. 12, no. 15, pp. 1755–1761, 2018.

[50] M. A. Soliman, H. M. Hasanien, and A. Alkuhayli, "Marine predators algorithm for parameters identification of triple-diode photovoltaic models," *IEEE Access*, vol. 8,

pp. 155 832–155 842, 2020.
[51] S. Mirjalili and A. Lewis, "The whale optimization algorithm," *Advances in engineering software*, vol. 95, pp. 51–67, 2016.
[52] M. Molga and C. Smutnicki, "Test functions for optimization needs," *Test functions for optimization needs*, vol. 101, p. 48, 2005.
[53] C. A. Floudas, P. M. Pardalos, C. Adjiman, W. R. Esposito, Z. H. Gümüs, S. T. Harding, J. L. Klepeis, C. A. Meyer, and C. A. Schweiger, *Handbook of test problems in local and global optimization*. Springer Science & Business Media, 2013, vol. 33.
[54] L. Dixon and D. Mills, "Effect of rounding errors on the variable metric method," *Journal of Optimization Theory and Applications*, vol. 80, no. 1, pp. 175–179, 1994.
[55] J. G. Digalakis and K. G. Margaritis, "On benchmarking functions for genetic algorithms," *International journal of computer mathematics*, vol. 77, no. 4, pp. 481–506, 2001.
[56] L. A. Rastrigin, "Systems of extremal control," *Nauka*, 1974.
[57] T. Bäck, "Artificial landscapes," in *Evolutionary Algorithms in Theory and Practice*. Oxford University Press.
[58] X.-S. Yang, "Firefly algorithm, stochastic test functions and design optimisation," *International journal of bio-inspired computation*, vol. 2, no. 2, pp. 78–84, 2010.
[59] K. Ishaque, Z. Salam, S. Mekhilef, and A. Shamsudin, "Parameter extraction of solar photovoltaic modules using penalty-based differential evolution," *Applied Energy*, vol. 99, pp. 297–308, 2012.
[60] Python Software Foundation, "Python 3.11 documentation," https://docs.python.org/3.11/, 2023, accessed: 28/04/2024.
[61] P. Virtanen, R. Gommers, T. E. Oliphant, M. Haberland, T. Reddy, D. Cournapeau, E. Burovski, P. Peterson, W. Weckesser, J. Bright *et al.*, "Scipy 1.0: fundamental algorithms for scientific computing in python," *Nature methods*, vol. 17, no. 3, pp. 261–272, 2020.
[62] S. Tosi, *Matplotlib for Python developers*. Packt Publishing Ltd, 2009.
[63] O. Ajetunmobi, "Improved parameter estimation of triple diode photovoltaic models," https://github.com/Shegzimus/Improved-Parameter-Estimation-of-Triple-Diode-Photovoltaic-Models, 2023, accessed: 28/02/2024.